

## EFFECTS OF NUMERICAL TREATMENT OF VISCOUS AND SURFACE TENSION FORCES ON PREDICTED INTERFACE MOTION

**Kosuke HAYASHI<sup>1\*</sup> and Akio TOMIYAMA<sup>1</sup>**

<sup>1</sup> Graduate School of Engineering, Kobe University, Rokkodai, Nada, Kobe 657-8501, JAPAN

\*Corresponding author, E-mail address: hayashi@mech.kobe-u.ac.jp

### ABSTRACT

Effects of treatment of viscous and surface tension forces on predictions of interface motion are investigated. The pressure and the normal component of surface tension force are calculated by using a ghost fluid method. The viscous and tangential surface tension forces are treated in two different ways: one is a smeared-out interface method and the other is the ghost fluid method (GFM). Linear shear flows, a single oscillating drop and a sinusoidal wave are simulated by using these methods. The main conclusions are as follows: (1) the velocity gradients in the two-phases near the interface are well predicted by using GFM, whereas the smeared-out interface method gives large errors, (2) the viscous damping of drop shape oscillation is overestimated by the smeared-out interface method, (3) both GFM and smeared-out interface method can qualitatively predict the damping of surface tension wave due to surfactant, whereas the latter method is apt to be numerically unstable.

### INTRODUCTION

Level set methods (Sussman et al., 1994) have been widely used for simulating multiphase flows such as bubbles, drops, interfacial waves and so on. The interface is modeled as a finite-thickness smeared-out interface in the original level set method. Therefore the surface tension force is calculated as a body force, by which the distribution of pressure is also smeared and a large spurious current is caused in the vicinity of interface. A sharp interface method for level set methods, which is known as a ghost fluid method (Kang et al., 2000), recently attracts much attention since this method can accurately deal with the jumps of physical quantities at the interface.

Most of recent level set methods utilize the ghost fluid method, GFM, to deal with the jumps of physical quantities, i.e. pressure, density and so on (Tanguy et al., 2007; Teigen et al., 2010; Bjorklund, 2009), whereas the viscous stress is often treated by means of the smeared-out interface method (Gibou et al., 2007; Tong & Wang, 2007; Yang & Stern, 2007; Desjardins et al., 2008; Hayashi & Tomiyama, 2012a, 2012b). This is mainly because the numerical implementation of the ghost fluid method in the viscous stress is more complicated compared with the smeared-out interface method. However accurate evaluation of the surface tension force and viscous stress at the interface is of great importance when the jump condition for the viscous stress includes the Marangoni force caused by the presence of surfactant, which drastically damps the surface tension wave.

Simulations of the motions of clean and contaminated interfaces are, therefore, carried out using the above-mentioned methods, i.e., the ghost fluid and smeared-out interface methods, to demonstrate how it is important to accurately evaluate the viscous and surface tension forces at the interface for obtaining good numerical predictions of the interface motion.

### NUMERICAL METHOD

#### Level Set Method

The interface is tracked by solving the following level set equation (Sussman et al., 1994):

$$\frac{\partial \phi}{\partial t} + \mathbf{V} \cdot \nabla \phi = 0 \quad (1)$$

where  $t$  is the time,  $\mathbf{V}$  the velocity, and  $\phi$  the level set function. The interface is represented by the zero-level set,  $\phi = 0$ . The unit normal to the interface and the curvature are given by

$$\mathbf{n} = \frac{\nabla \phi}{|\nabla \phi|} \quad (2)$$

$$\kappa = -\nabla \cdot \frac{\nabla \phi}{|\nabla \phi|} \quad (3)$$

The level set function will not be a distance function after the advection of  $\phi$ . The following re-initialization equation is, therefore, solved at each time step to recover the property of  $\phi$  as the distance function (Sussman et al., 1994):

$$\frac{\partial \phi}{\partial \tau} = \text{sign}(\phi)[1 - |\nabla \phi|] \quad (4)$$

where  $\tau$  is the pseudo time and  $\text{sign}(\phi)$  the smoothed sign function defined by  $\text{sign}(\phi) = \phi / \sqrt{\phi^2 + \Delta x^2}$  and  $\Delta x$  is the cell width in the  $x$  direction.

As is well known, the re-initialization slightly changes the interface position, and therefore, the mass conservation is deteriorated. Meier's global correction method (Meier, 2000) is utilized in this study to assure the mass conservation.

#### Smeared-out Interface Method for Viscous Stress

A numerical method proposed in our previous study (Hayashi & Tomiyama, 2012a; 2012b) is used as a smeared-out interface method for the viscous stress.

Details and validations of the method can be found in the literature.

The continuity and momentum equations for incompressible Newtonian fluids based on one-fluid formulation are given by

$$\nabla \cdot \mathbf{V} = 0 \quad (5)$$

$$\frac{\partial \mathbf{V}}{\partial t} + \mathbf{V} \cdot \nabla \mathbf{V} = -\frac{1}{\rho} \nabla P + \frac{1}{\rho} \nabla \cdot \mu [\nabla \mathbf{V} + (\nabla \mathbf{V})^T] + \mathbf{g} + \frac{1}{\rho} [\sigma \kappa \mathbf{n} + \nabla_S \sigma] \delta \quad (6)$$

where  $\rho$  is the density,  $P$  the pressure,  $\mu$  the viscosity,  $\mathbf{g}$  the acceleration of gravity,  $\sigma$  the surface tension,  $\nabla_S (= \nabla - \mathbf{n} \cdot \nabla)$  the surface gradient operator,  $\delta$  the delta function, which is non-zero only at the interface, and the superscript  $T$  denotes the transpose. The term,  $(\nabla_S \sigma) \delta$ , is the tangential component of surface tension force, i.e., the Marangoni force.

The ghost fluid method (Kang et al., 2000) is adopted to evaluate the normal component of the surface tension force. The momentum equation without the pressure gradient and the normal component of surface tension force is solved to obtain a temporary velocity,  $\mathbf{V}^*$ :

$$\mathbf{V}^* = \mathbf{V}^n + \Delta t \left[ \begin{array}{c} -\mathbf{V} \cdot \nabla \mathbf{V} + \frac{1}{\rho} \nabla \cdot \mu [\nabla \mathbf{V} + (\nabla \mathbf{V})^T] \\ + \mathbf{g} + \frac{(\nabla_S \sigma) \delta}{\rho} \end{array} \right]^n \quad (7)$$

where the superscript  $n$  denotes the time step and  $\Delta t$  is the time step size, i.e.  $t = n\Delta t$ . The density  $\rho$  and viscosity  $\mu$  are given by

$$\rho = \rho^+ + (\rho^+ - \rho^-) H_\varepsilon(\phi) \quad (8)$$

$$\mu = \mu^+ + (\mu^+ - \mu^-) H_\varepsilon(\phi) \quad (9)$$

where the superscripts  $+$  and  $-$  denote the values of the phases of  $\phi > 0$  and  $\phi < 0$ , respectively, and  $H_\varepsilon(\phi)$  is the smoothed Heaviside function given by

$$H_\varepsilon(\phi) = \begin{cases} 0 & \text{for } \phi < -\varepsilon \\ \frac{1}{2} + \frac{\phi}{2\varepsilon} + \frac{1}{2\pi} \sin\left(\frac{\pi\phi}{\varepsilon}\right) & \text{for } |\phi| \leq \varepsilon \\ 1 & \text{for } \phi > \varepsilon \end{cases} \quad (10)$$

Here the parameter  $\varepsilon$  is set at  $1.5\Delta x$ , where  $\Delta x$  is the cell size.

The CSF (continuum surface force) model (Brackbill et al., 1992) is utilized to evaluate the Marangoni force:

$$(\nabla_S \sigma) \delta = \left[ \nabla \sigma - \frac{\nabla \phi}{|\nabla \phi|} \left( \frac{\nabla \phi}{|\nabla \phi|} \cdot \nabla \sigma \right) \right] \delta_\varepsilon(\phi) \quad (11)$$

where  $\delta_\varepsilon(\phi)$  is the smoothed delta function given by

$$\delta_\varepsilon(\phi) = \begin{cases} \frac{1}{2\varepsilon} \left[ 1 + \cos\left(\frac{\pi\phi}{\varepsilon}\right) \right] & \text{for } |\phi| < \varepsilon \\ 0 & \text{otherwise} \end{cases} \quad (12)$$

The pressure at the new time step  $n+1$  is obtained by solving the following Poisson equation:

$$\nabla \cdot \frac{\Delta t}{\rho} \nabla P^{n+1} = \nabla \cdot \mathbf{V}^* \quad (13)$$

The normal component of surface tension force is taken into account when evaluating the pressure gradient in the above equation. Let us consider the following case: the center of the cell  $i$  belongs to the phase of  $\phi < 0$  and that of the neighboring cell,  $i+1$ , in the  $x$  direction belongs to the phase of  $\phi > 0$ . In this case, the term,  $\rho^{-1} \partial P / \partial x|_{i+1/2}$ , at the cell face  $i+1/2$  is evaluated as

$$\frac{1}{\rho} \frac{\partial P^{n+1}}{\partial x} \Big|_{i+1/2} = \frac{1}{\rho^*} \frac{P_{i+1}^{n+1} - P_i^{n+1}}{\Delta x} - \frac{1}{\rho^*} \frac{[P]_{int}}{\Delta x} \quad (14)$$

where the subscript  $int$  denotes the interface,  $[X]_{int}$  is the jump at the interface  $X^+ - X^-$  and the mixture density  $\rho^*$  is given by

$$\rho^* = (1 - \theta) \rho^- + \theta \rho^+ \quad (15)$$

Here the fraction  $\theta$  is

$$\theta = \frac{|\phi_{i+1}|}{|\phi_i| + |\phi_{i+1}|} \quad (16)$$

The second term in the R.H.S. of Eq. (14) expresses the contribution of the pressure jump due to the surface tension force in the normal direction, i.e.,

$$[P]_{int} = P^+ - P^- = \sigma \kappa \quad (17)$$

Then  $\mathbf{V}^*$  is projected onto the divergence-free vector  $\mathbf{V}^{n+1}$ :

$$\mathbf{V}^{n+1} = \mathbf{V}^* - \frac{\Delta t}{\rho} \nabla P^{n+1} \quad (18)$$

The pressure gradient in the above equation is evaluated in the same way as in Eq. (14).

#### Ghost Fluid Method for Viscous Stress

The jump condition for the tangential stresses at the interface is given by

$$[t_i \tau_{ij} n_j]_{int} = t_i \frac{\partial \sigma}{\partial x_i} \quad (19)$$

$$[s_i \tau_{ij} n_j]_{int} = s_i \frac{\partial \sigma}{\partial x_i} \quad (20)$$

where  $t_i$  and  $s_i$  are the unit tangents to the interface, for which  $t_i s_i = n_i t_i = n_i s_i = 0$ , and  $\tau_{ij}$  the viscous stress tensor defined by

$$\tau_{ij} = \mu \left( \frac{\partial V_i}{\partial x_j} + \frac{\partial V_j}{\partial x_i} \right) \quad (21)$$

Rearranging Eqs. (19) and (20) by making use of

$$\left[ t_j \frac{\partial V_i}{\partial x_j} n_i \right]_{int} = 0 \quad , \quad \left[ s_j \frac{\partial V_i}{\partial x_j} n_i \right]_{int} = 0 \quad \text{and}$$

$$\left[ n_j \frac{\partial V_i}{\partial x_j} n_i \right]_{int} = 0 \quad \text{yields the jump in } \mu \nabla V:$$

$$J_{ij} = \left[ \mu \frac{\partial V_i}{\partial x_j} \right]_{int} = [\mu]_{int} t_i t_m \frac{\partial V_m}{\partial x_j} + [\mu]_{int} s_i s_m \frac{\partial V_m}{\partial x_j}$$

$$+ [\mu]_{int} n_i n_j \left( n_m n_n \frac{\partial V_n}{\partial x_m} \right) - [\mu]_{int} t_i n_j \left( t_m n_n \frac{\partial V_m}{\partial x_n} \right) \quad (22)$$

$$- [\mu]_{int} s_i n_j \left( s_m n_n \frac{\partial V_m}{\partial x_n} \right) - n_j \frac{\partial \sigma}{\partial x_i}$$

The jump,  $J_{ij}$ , is used for evaluating the viscous stresses at the interface between computational grid points including. For instance, if the cell face at  $i + 3/2$  belongs to the phase of  $\phi > 0$  and those at  $i + 1/2$  and  $i - 1/2$  belong to the phase of  $\phi < 0$  (the interface lies between  $i + 3/2$  and  $i + 1/2$ ), the viscous stresses,  $\mu \partial u / \partial x|_{i+1}$  and  $\mu \partial u / \partial x|_i$  are evaluated as

$$\mu \frac{\partial u}{\partial x} \Big|_{i+1} = \hat{\mu} \frac{u_{i+3/2} - u_{i+1/2}}{\Delta x} - \frac{\hat{\mu}}{\mu^+} J_{xx} \theta \quad (23)$$

$$\mu \frac{\partial u}{\partial x} \Big|_i = \mu^- \frac{u_{i+1/2} - u_{i-1/2}}{\Delta x} \quad (24)$$

where

$$\hat{\mu} = \frac{\mu^+ \mu^-}{\mu^+ (1 - \theta) + \mu^- \theta} \quad (25)$$

When applying the ghost fluid method to the pressure, the jump,  $[P]_{int}$ , in Eq. (17) is rewritten as

$$[P]_{int} = \sigma \kappa + 2[\mu]_{int} n_i n_j \frac{\partial V_i}{\partial x_j} \quad (26)$$

Details can be found in Kang et al. (2000).

### Calculation of Surfactant Concentration

The transport equation of surfactant in the continuous phase and that at the interface are given by (Levich, 1962; Stone, 1990)

$$\frac{\partial C}{\partial t} + \mathbf{V} \cdot \nabla C = \nabla \cdot D_C \nabla C \quad (27)$$

$$\frac{\partial \Gamma}{\partial t} + \nabla_S \cdot \Gamma \mathbf{V} = \nabla_S \cdot D_S \nabla_S \Gamma + \dot{S}_\Gamma \quad (28)$$

where  $C$  is the surfactant concentration in the continuous phase,  $\Gamma$  the surfactant concentration at the interface,  $D_C$  and  $D_S$  are the diffusion coefficient in the continuous phase and that at the interface, respectively, and  $V_S$  the tangential component of  $\mathbf{V}$ . The source term  $\dot{S}_\Gamma$  is the molar flux from the continuous phase to the interface due to the adsorption and desorption. In this study, the

adsorption and desorption of surfactant are neglected, i.e.  $\dot{S}_\Gamma = 0$ , for simplicity. Equation (27) is, therefore, not solved. The method for solving Eq. (27) and the treatment of  $\dot{S}_\Gamma$  are described in Hayashi & Tomiyama (2012a).

The molar concentration  $\Gamma$  at the interface is extrapolated into both phases by solving the following equation (Xu & Zhao, 2003):

$$\frac{\partial \Gamma}{\partial \tau} + \text{sign}(\phi) \mathbf{n} \cdot \nabla \Gamma = 0 \quad (29)$$

The extrapolated  $\Gamma$  satisfies  $\mathbf{n} \cdot \nabla \Gamma = 0$  in the two phases and at the interface. Hence  $\nabla_S \Gamma = \nabla \Gamma - \mathbf{nn} \cdot \nabla \Gamma = \nabla \Gamma$ . Once  $\Gamma$  is extrapolated, the transport equation of  $\Gamma$ , Eq. (28), can be solved with any difference schemes. A correction method (Xu et al., 2006) for keeping the total amount of  $\Gamma$  is adopted.

The surface tension  $\sigma$  is calculated using

$$\sigma(\Gamma) = \sigma_0 \left[ 1 + \eta \ln \left( 1 - \frac{\Gamma}{\Gamma_{max}} \right) \right] \quad (30)$$

where  $\sigma_0$  is the surface tension of clean interface,  $\eta$  the damping coefficient, and  $\Gamma_{max}$  the saturation value of  $\Gamma$ .

The above-mentioned methods use the staggered variable arrangement, i.e., the components of vectors are located at the cell face, whereas the scalars are located at the cell center.

## RESULTS AND DISCUSSION

### Linear Shear Flow

Linear shear flow in two parallel walls shown in Fig. 1 is calculated. The horizontal velocity component in the absence of Marangoni force at the steady state is given by

$$u(y) = \begin{cases} \frac{U - u_{int}}{h} (y - y_{int}) + u_{int} & \text{for } y \geq y_{int} \\ \frac{U + u_{int}}{H - h} y - U & \text{for } y < y_{int} \end{cases} \quad (31)$$

where  $y$  is the vertical coordinate and the interface velocity  $u_{int}$  is given by

$$u_{int} = \frac{\mu^* (H - h) - h U}{\mu^* (H - h) + h} \quad (32)$$

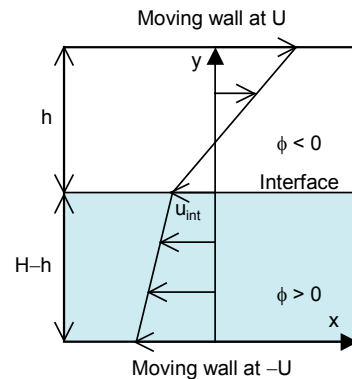


**Figure 1:** Computational domain for linear shear flow simulation

where  $\mu^*$  is the viscosity ratio defined by  $\mu^* = \mu^-/\mu^+$ . The right and left boundaries are periodic. The top and bottom boundaries are moving walls at  $U$  and  $-U$ , respectively. The number of computational cells in the  $x$  and  $y$  directions are 20 and 20, respectively. The other conditions are as follows:  $U = 1$ ,  $H = 20$ ,  $h = 9.75$ ,  $\mu^+ = 0.01$ ,  $\mu^- = 5 \times 10^{-5}$  and  $\mu^* = 5 \times 10^{-3}$ .

Horizontal velocity predicted using the smeared-out method is compared with the analytical solution in Fig. 2. Due to the large viscosity difference between the two phases, the velocity gradient for  $y < y_{int}$  is very small. The smeared-out interface method causes the large error in velocity gradient near the interface. This is because the mixture viscosity in the phase of  $\phi < 0$  is evaluated much higher than the actual value,  $\mu^-$ , due to the arithmetic mean, Eq. (9). The velocity predicted using GFM for viscous stress is also shown in the figure. The agreement between the GFM prediction and the analytical solution is very good.

When the Marangoni force is non-zero and is constant over the whole interface, the interface velocity is given by

$$u_{int} = \frac{[\mu^*(H-h) - h]U + \frac{h(H-h)}{\mu^+} \frac{\partial \sigma}{\partial x}}{\mu^*(H-h) + h} \quad (33)$$

Velocity profiles predicted with  $\partial \sigma / \partial x = -0.001$  are shown in Fig. 3. The effect of the Marangoni force on velocity

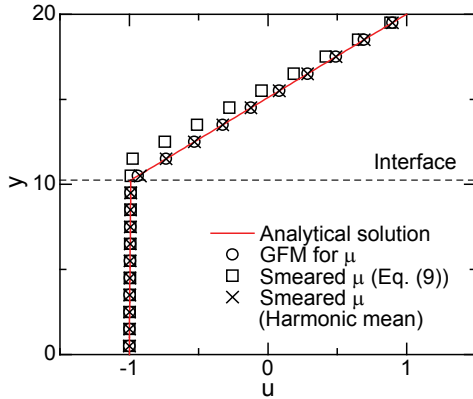


**Figure 2:** Horizontal velocities of linear shear flows predicted with smeared-out and ghost fluid methods for viscous stress

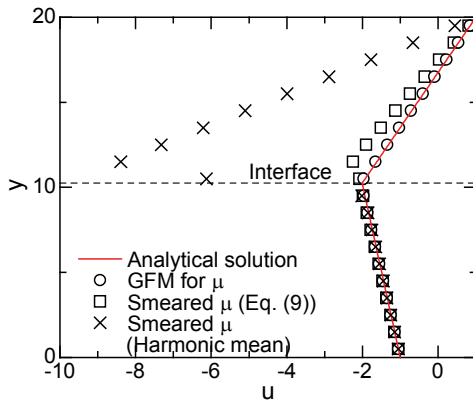


**Figure 3:** Horizontal velocities of linear shear flows predicted with smeared-out and ghost fluid methods for viscous stress. The Marangoni force,  $\partial \sigma / \partial x = -0.001$ , is adopted to the interface.

profile is well predicted with both methods, i.e., the Marangoni force directing toward the negative  $x$  makes  $u$  lower compared to the case of clean interface. GFM, however, gives the more accurate prediction.

It is known that the harmonic mean,  $\mu = H_e/\mu^+ + (1-H_e)/\mu^-$ , gives better evaluations of the viscous stress than Eq. (9) in simulations of the smeared-out interface method (Prosperetti, 2002). This is clearly seen in Fig. 2. However it should be noted that the harmonic mean causes large errors for the flow with the Marangoni force as shown in Fig. 3. As pointed out by Hayashi & Tomiyama (2012a), the harmonic-mean, which was derived from the jump condition of the tangential viscous stress without considering the Marangoni force, cannot correctly deal with the jump condition with the Marangoni force  $[t_i \tau_{ij} n_j]_{int} = t_i \partial \sigma / \partial x_i$ .

### Oscillating Drop

A single drop oscillated by surface tension force is simulated. The numerical conditions are the same as those used in Torres & Brackbill (2000). The computational domain is square and its width is 20. The initial drop shape is an ellipsoid given by

$$\left(\frac{x-x_0}{3}\right)^2 + \left(\frac{y-y_0}{2}\right)^2 - 1 = 0 \quad (34)$$

where  $x_0$  and  $y_0$  are the coordinates of the domain center. The drop is initially at rest. The number of computational cells in each direction is 64. The physical properties are  $\rho^+ = 1$ ,  $\rho^- = 0.01$ ,  $\mu^+ = 0.01$ ,  $\mu^- = 5 \times 10^{-5}$  and  $\sigma_0 = 1$ . The interface is assumed clean. The gravity is absent.

The drop motion and velocity field predicted by using the smeared-out interface method is shown in Fig. 4. The left and right edges of drop are pulled by strong surface tension toward the drop center and the top and bottom edges are pushed out ( $t = 2$  and 4). The drop then starts to deform in the opposite direction at  $t = 6$  and reaches almost the same shape as the initial condition at  $t = 10$ . The drop repeats the similar shape oscillation, whereas the degree of deformation gradually attenuates with time due to the viscous dissipation. The velocity profile seems to be smooth and no remarkable spurious currents are found as in predictions with the CSF model for the pressure and normal component of surface tension force (e.g. Tong & Wang, 2007). Predictions of the drop shape and velocity field by GFM are similar to those by the smeared-out interface method as shown in Fig. 5.

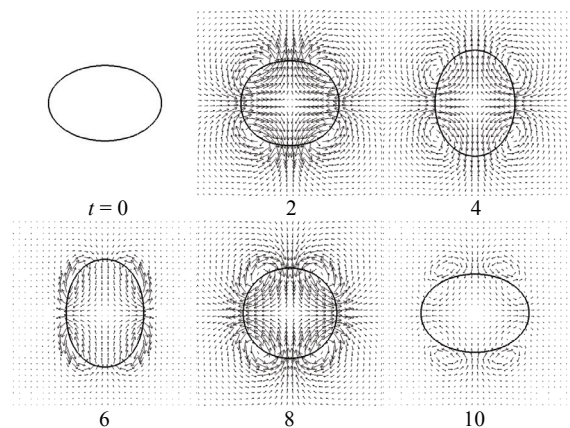


**Figure 4:** Shape and velocity field of oscillating drop simulated with smeared-out interface method

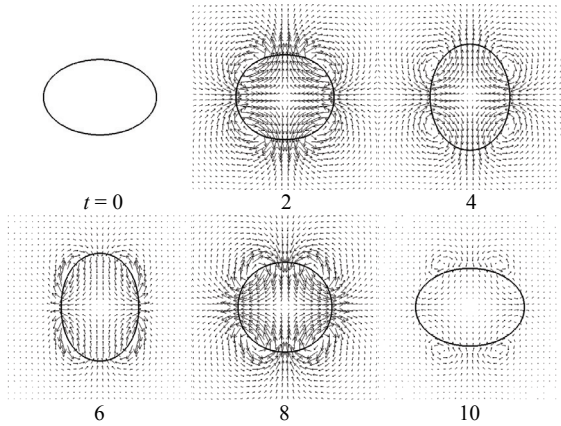


**Figure 5:** Shape and velocity field of oscillating drop simulated with GFM for viscous stress

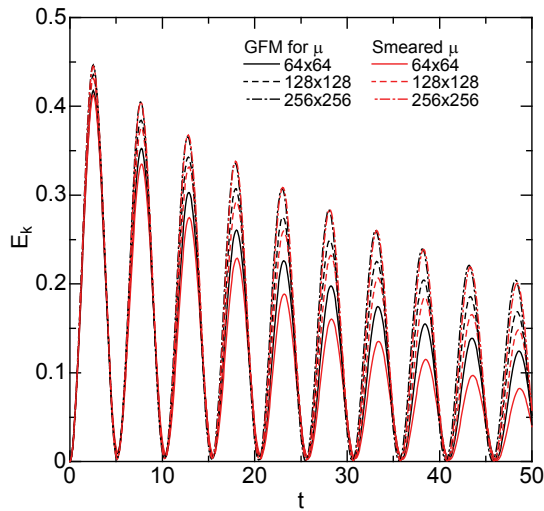


**Figure 6:** Total kinetic energy of two phases for single oscillating drop problem

The total kinetic energy in the whole computational area,  $S$ , is evaluated as

$$E_K = \iint_S \frac{1}{2} \rho V^2 dS \quad (35)$$

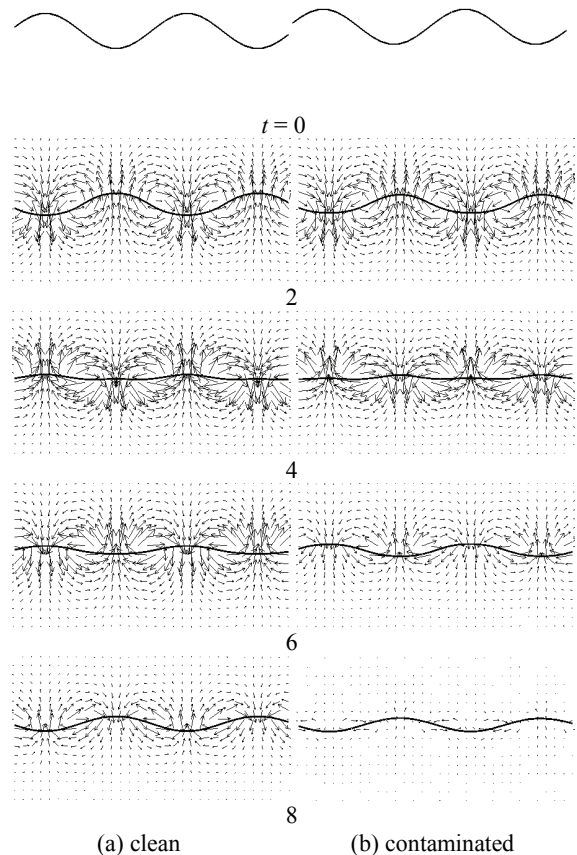
A comparison of  $E_K$  between GFM and the smeared-out interface method is shown in Fig. 6. The kinetic energy oscillates due to drop oscillation and the amplitude of oscillation decreases with time due to the viscous dissipation. With the spatial resolution,  $64 \times 64$ ,  $E_K$  of both methods are almost the same in the early stage of the oscillation, whereas the prediction of the smeared-out interface method becomes lower and lower than that of GFM. This means that the viscous dissipation is larger in the smeared-out interface method. As discussed in the previous section, the smeared-out interface method gives large errors in the velocity gradient (viscous stress) near the interface. This error is expected to decrease as the spatial resolution increases because the increase in spatial resolution decreases the thickness of smeared-out interface. Comparisons of  $E_K$  for higher spatial resolutions are also shown in the figure. The difference in  $E_K$  between the two methods decreases as the spatial resolution increases. With the highest spatial resolution, they give almost the same

solution. At low spatial resolutions, GFM gives better predictions than the smeared-out interface method.

### Surface Tension Wave

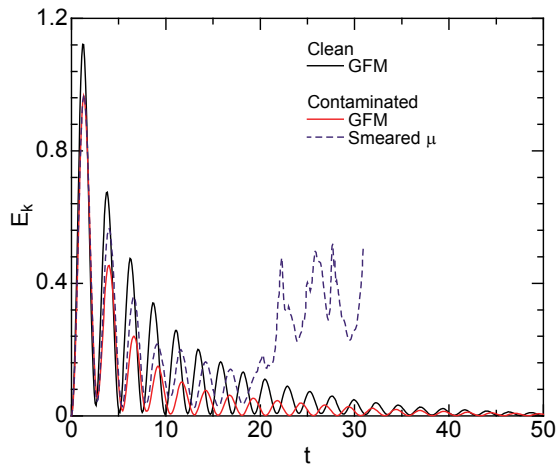
A surface tension wave at the interface is simulated. The computational domain is rectangular, whose width and height are 10 and 20. The right and left boundaries are periodic. The top and bottom boundaries are continuous outflow and no-slip, respectively. The numbers of cells in the  $x$  and  $y$  directions are 32 and 64, respectively. The initial interface shape is sinusoidal, i.e.  $y = A \sin(2\pi x/\lambda)$  where  $A = 2\Delta x$  and  $\lambda = 5$ . Both fluids are initially at rest. The gravity is not considered in the simulation. Hence the force driving interface motion is only the surface tension force. The fluid properties are the same as those in the oscillating drop. In a contaminated case,  $\eta = 0.2$  and  $\Gamma = 0.1$  over the whole surface at  $t = 0$  are used. The diffusion of  $\Gamma$  is neglected.

Figure 7 shows motions of clean and contaminated interfaces and velocity fields predicted using GFM. The attenuation of oscillating motion is much larger in the contaminated case than in the clean interface case because of the damping due to the Marangoni force (Landau & Lifshitz, 1987). The total kinetic energies are compared in Fig. 8, which clearly shows the damping effect. The total kinetic energy predicted using the smeared-out interface method is also shown in the figure. The damping effect due to surfactant can also be predicted, whereas the prediction becomes unstable as the time proceeds and the numerical simulation diverges at  $t \sim 30$ . This is because



**Figure 7:** Surface tension waves on clean and contaminated interfaces. Both results are obtained using GFM.

the Marangoni force calculated with Eq. (11) excessively accelerates the lighter fluid and makes the velocity component tangent to the interface large. This instability might be mitigated by multiplying Eq. (11) by  $2\rho/(\rho^+ + \rho^-)$  as proposed in the CSF model for the term  $\sigma\kappa\mathbf{n}\delta$ . The effects of this modification will be investigated in the near future.



**Figure 8:** Total kinetic energy of two fluids for sinusoidal surface tension wave

## CONCLUSION

Effects of the treatment of viscous stress and Marangoni force at the interface on predicted interface motion were investigated. The numerical method was based on a level set method. The pressure and normal component of the surface tension force were computed by using a ghost fluid method. Two different approaches were examined for the viscous stress and Marangoni force, i.e., the smeared-out interface method and the ghost fluid method. Linear shear flows including a flat interface and single oscillating drop were simulated as test cases. As a result, the following conclusions were obtained:

- (1) The velocity gradients in the two-phases near the interface are accurately predicted by using GFM, whereas the smeared-out interface method gives a large error in the velocity gradient.
- (2) The viscous damping of drop shape oscillation is overestimated by the smeared-out interface method, especially when the spatial resolution is low, that is, when the thickness of the smeared-out interface is thick.
- (3) Both GFM and smeared-out interface method can qualitatively predict the damping of surface tension wave due to surfactant. The latter method, however, is apt to be numerically unstable.

## ACKNOWLEDGEMENT

This work has been supported by the Japan Society for the Promotion of Science (JSPS) (grants-in-aid for scientific research (B) (24360070) and for young scientists (B) (23760160)).

## REFERENCES

BJORKLUND, E., (2009), "The level-set method applied to droplet dynamics in the presence of an electric field", *Computers & Fluids*, 38, 358-369.

BRACKBILL, J. U., KOTHE, D. B. and ZEMACH, C., (1992), "A continuum method for modeling surface tension", *Journal of Computational Physics*, vol. 100, pp. 335-354.

DESJARDINS, O., MOUREAU, V. and PITTSCH, H., (2008), "An accurate conservative level set/ghost fluid method for simulating turbulent atomization", *Journal of Computational Physics*, 277, 8395-8416.

GIBOU, F., CHEN, L., NGUYEN, D. and BANERJEE, S., (2007), "A Level Set based Sharp Interface Method for the Multiphase Incompressible Navier-Stokes Equations With Phase Change", *Journal of Computational Physics*, 222, 536-555.

HAYASHI, K. and TOMIYAMA, A., (2012a), "Effects of surfactant on terminal velocity of a Taylor bubble in a vertical pipe", *International Journal of Multiphase Flow*, 39, 78-87.

HAYASHI, K., KURIMOTO, R., HOSOKAWA, S. and TOMIYAMA, A., (2012b), "Effects of surfactant on the motion of bubbles in linear shear flows", *In Proceedings of the Japan-U.S. seminar on Two-Phase Flow Dynamics 2012, Japan*.

KANG, M., FEDKIW, R. P. and LIU, X.-D., (2000), "A boundary condition capturing method for multiphase incompressible flow", *Journal of Scientific Computing*, 15, 323-360.

LANDAU, L. D., LIFSHITZ, E. M., (1987), *Fluid Mechanics*, Pergamon Press.

LEVICH, V. G., (1962), *Physicochemical hydrodynamics*, Prentice Hall.

MEIER, M., (2000), "Towards a DNS of multiphase flow", Technical Report No. LKT-01-00, *Laboratorium für Kerntechnik Institut für Energietechnik*, ETH Zurich.

PROSPERETTI, A., (2002), "Drop-surface interactions", ed. Rein, M., Springer.

STONE, H. A., (1990), "A simple derivation of the time-dependent convective-diffusion equation for surfactant transport along a deforming interface", *Physics of Fluids A*, 2, 111-112.

SUSSMAN, M., SMERKA, P. and OSHER, S., (1994), "A level set approach for computing solutions to incompressible two-phase flow", *Journal of Computational Physics*, 114, 146-159.

TANGUY, S., MENARD, T. and BERLEMONT, A., (2007), "A Level Set Method for vaporizing two-phase flows", *Journal of Computational Physics*, 221, 837-853.

TEIGEN, K. E., LERVAG, K. Y. and MUNKEJORD, S. T., (2010), "Sharp Interface Simulations of surfactant-covered drops in electric fields", *In Proceedings of the fifth European Conference on Computational Fluid Dynamics, ECCOMAS CFD 2010*.

TONG, A. Y. and WANG, Z., (2007), "A numerical method for capillarity-dominant free surface flows", *Journal of Computational Physics*, 221, 506-523.

TORRES, D. J., BRACKBILL, J. U., (2000), The Point-Set Method: Front-Tracking, *Journal of Computational Physics*, 165, 620-644.

without Connectivity

YANG, J. and STERN, F., (2007), "A Sharp Interface Method for Two-Phase Flows Interacting with Moving Bodies", *In Proceedings of the 18th AIAA Computational Fluid Dynamics Conference*.

XU, J.-J. and ZHAO, H.-K., (2003), "An Eulerian formulation for solving partial differential equations along moving interface", *Journal of Scientific Computing*, 19, 573-594.

XU, J.-J., LI, Z., LOWENGRUB, J. and ZHAO, H., (2006), "A level-set method for interfacial flows with surfactant", *Journal of Computational Physics*, 212, 590-616.